ID-1101

CHAMBERCORE TESTING AND ANALYSIS

Julie Q. Wang, Akira Kuraishi and Stephen W. Tsai
Dept. of Aeronautics and Astronautics
Stanford University
Stanford, CA 94305 U.S.A.

Peter M. Wegner
Air Force Research Lab/VSSV
Kirtland AFB, NM 87117 U.S.A.

ABSTRACT: Grid structures made of composite materials offer high stiffness and strength at low mass that are competitive with traditional composite laminates. We have been studying composite grid structures as high performance structures for various applications. Chambercore is one type of composite grid structure we have developed for aerospace applications that could replace conventional sandwich structures. This paper presents an experimental investigation and a preliminary analytical study of flat chambercore panels, that are essential for understanding their behavior and design.

KEYWORDS: grid structure, chambercore, 4-point bending, compression, buckling mode

INTRODUCTION

Chambercore panels are made of stacked composite tubes which are then sandwiched by composite face sheets. The inner tubes have a square cross section for flat applications and a fan-shaped cross section for cylindrical applications. The sidewalls of the tubes act as ribs to separate the upper and lower skins, similar to a honeycomb core. The open space or "chambers," that the tubes create, can be used for acoustic suppression or thermal insulation, making this structure suitable for launch vehicle applications.

Flat Chambercore panels with two different cell sizes of square cross sections were studied. These panels were fabricated by the Air Force Research Lab. The cell size of the Chambercore panels was 4 cm by 1.3 cm for the small size and 4.4 cm by 1.9 cm for the larger size. The panels were made of IM7/8552 prepreg. The cores and face sheets are one-step co-cured with the use of an expanding rubber mold. The ply orientation of the face sheets is $[0/90]_s$ and of the cells is $[0/90/9090/90]_T$. The "lengthwise-direction" is along the length of the tube and the "transverse-direction" is across the width of the tube. The Structures and Composites Lab at Stanford University performed 4 types of tests: transverse 4-point bending, short lengthwise 4-point bending, compression/buckling, and long lengthwise 4-point bending tests.

1) Transverse 4-point bending test

Small cell Chambercore panels were used for this test. The support span of the test setup was 4 times the cell width while the load span used twice the cell width. Total load and displacement at loading points were measured (Figure 1).

Three specimens were tested and failed. The same failure mode was observed in each case (Appendix 1). The delamination started from the corner of the cell between the juncture of the cell wall and the face-sheet near the loading points (Appendix 2).

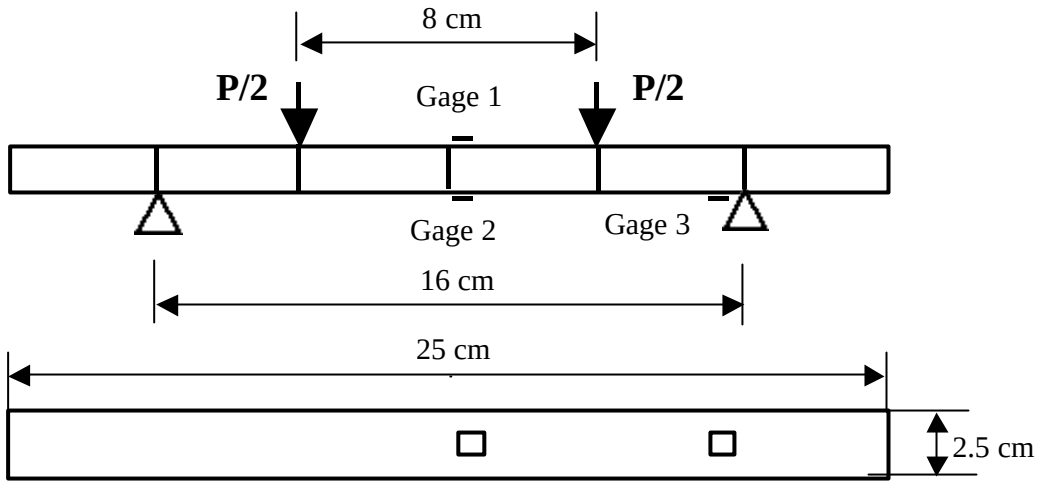

Figure 1 Transverse 4-Point Bending Test

Three strain gages were attached on the first specimen as shown in Figure 1. The strain measurements correlated well with results from the finite element analysis (FEA) using the commercial code ANSYS (Appendix 3).

	Strains per unit load (1/N)	
	Experiment	FEA
Location 1	-8.0E-7	-1.3E-6
Location 2	7.9E-7	1.3E-6
Location 3	9.6E-7	1.2E-3

Displacements per unit load (cm/N)	
Experiment	FEA
1.0E-3	1.3E-3

2) Short lengthwise 4-point bending test

Small cell Chambercore panels that were one full cell wide were used for this test. The support span was set to 11.4 cm and the load span to 3.8 cm for the test (Figure 2). The ratio of the length to thickness of the specimen suggests that a 4-point bending test in this configuration is actually a combination of a bending and short beam shear test.

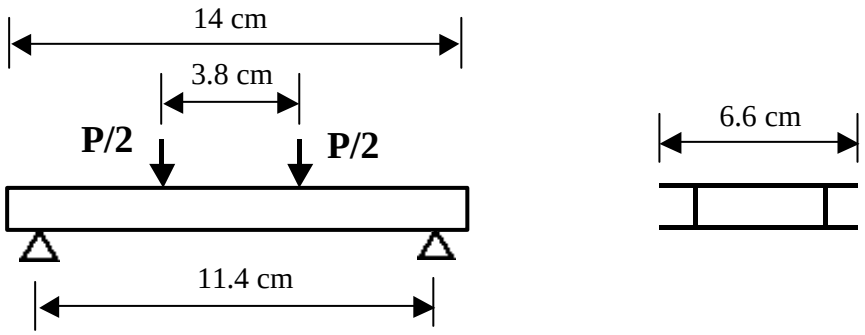

Figure 2 Short Lengthwise 4-Point Bending Test

Two specimens were tested and both failed in the same failure mode (Appendix 4). First, the ribs under the loading point started to buckle, then, the cell began to delaminate from the two face sheets. Finally, the face sheet on the compression side broke and the load dropped sharply (Appendix 5). The experimental results show good agreement with the FEA results (Appendix 6).

Displacement over Load (cm/N)	
Experiment	FEA
2.0E-5	1.8E-5

3) Compression/Buckling test

A specimen with two full small cells and a 1.27 cm flange on each side was used for a panel buckling test (Figure 3). Four strain gages were attached near the middle of the cells in regions where peak strains were expected to occur after buckling. We put inserts in the flanges on each side and clipped the flanges with paper clips in order to constrain these two sides. Otherwise, these two sides would buckle prior to the cells' buckling under compression (Appendix 7). An FEA model was developed to predict the buckling behavior of the panels (Appendix 8).

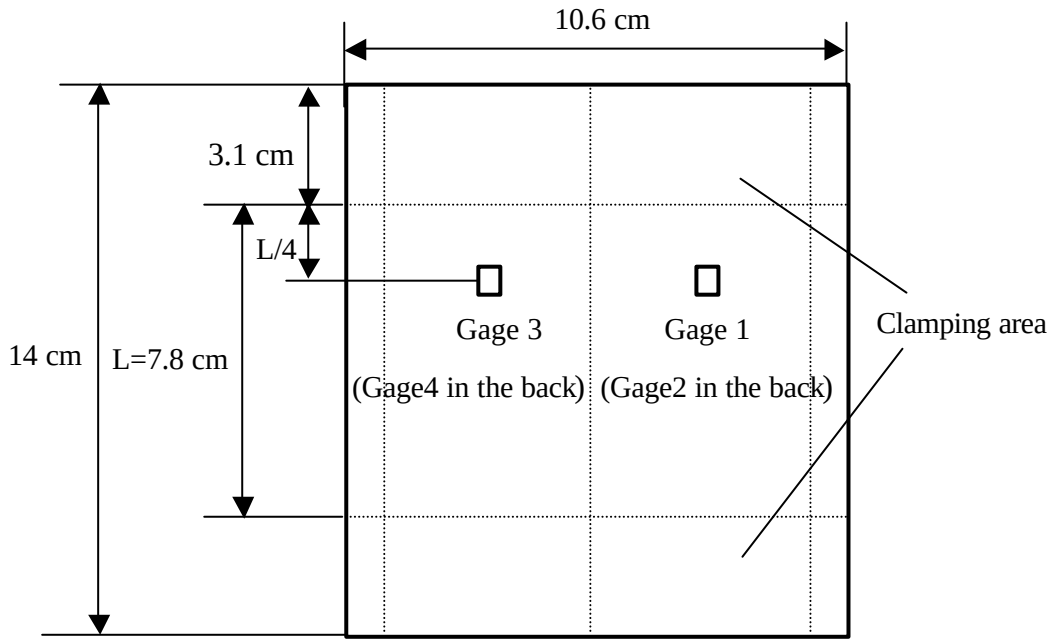

Figure 3 Panel Buckling Test

Load, displacement, and strain were measured during the test (Appendix 9 & 10). For better comparison, we used the middle portion of the data after the top and bottom of the specimen "fully" contacted the fixture and before buckling. The specimen started to buckle after the compressive load reached approximately 49,000 N. The measured strains were close to the FEA predictions, however the buckling load measured was lower than those calculated by the model. The buckling mode observed compared well with the second mode in the FEA prediction. The predicted buckling load for the first mode was around 80,000 N and the second mode was 82,000 N. There were some differences in the boundary conditions between the test and the analysis, which influenced these results. In the analysis, the four sides were constrained. In our test, both the upper and lower sides of the specimen were clamped by the shims of the fixture, but the fixture could not prevent the surfaces from deflecting inwards.

Small gaps between the shims of the fixture and the surfaces of the specimen were observed after buckling, although the gaps are too small to be seen from the pictures (Appendix 11).

Strains per Unit Load (1/N)

	Experiment	FEA
Location 1	4.3E-08	5.4E-08
Location 2	4.9E-08	5.4E-08
Location 3	4.0E-08	5.4E-08
Location 4	4.5E-08	5.4E-08

Buckling Load (N)

Experiment	FEA
49,000	82,000

The test was stopped when the load reached 111,000 N. However, the specimen did not break. After unloading, the load and strains returned almost to zero or their original values. This demonstrates the "gentle buckling behavior" of these grid structures. In other words, these grid structures often do not fail catastrophically when they buckle, they continue to carry a significant amount of compressive loading after the first buckling mode is reached. This characteristic could be used to design very safe and reliable structures.

4) Long Lengthwise 4-Point Bending

Three Chambercore panels/beams 61cm long with one full big cell were used for this test. The test was set up with the support span 53.3 cm and the load span 17.8 cm. One strain gage was attached on the skin of tensile side and in the middle area of the two ribs of the first specimen. Load and displacement at the loading points and strain data from the gages were recorded during the test (Figure 4). Each of the three specimens failed in the same failure mode and their failure loads were very similar (Appendix 12 & 13).

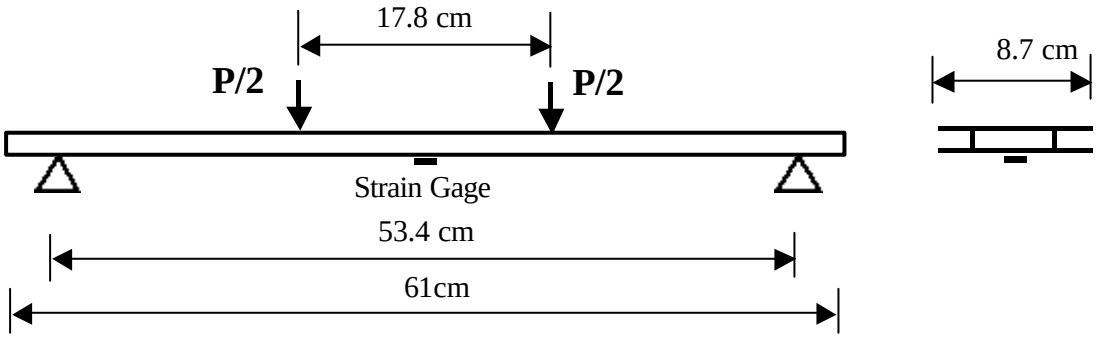

Figure 4 Long Lengthwise 4-Pint Bending Test

The upper (compression side) skin between the two loading points of the specimen started to buckle at a load of about 2,700 N. The buckling propagated from the two sides to the central part of the upper skin as the applied load increased. When the load reached the peak failure value, the upper skin broke, and then the ribs broke right under the loading points. The failure loads were approximately 6,200 N.

Following the long lengthwise 4-point bending tests, finite element analyses were performed (Appendix 14 & 15). The predicted buckling load was higher than the actual buckling load mainly due to the difficulty in modeling the true experimental boundary conditions. The difference in the stiffness can be attributed to the wide variation in the thickness of the specimens and the differences in the boundary conditions. The calculations were all based on a ply thickness of 0.15 cm, while the actual ply thickness ranged from 0.11 cm to 0.15 cm.

This variation in thickness was primarily due to the difference in compaction during curing. In this case, the in-plane propertis of the laminate will not vary significantly, but the bending properties vary according to the ply thickness.

	Displacement/load (cm/N)	**Strain/load (1/N)**	**Buckling load (N)**
Experiment	2.2E-4	7.1E-7	2,900
FEA	1.9E-4	6.3E-7	4,900

Conclusion

Our experiments reveal the complex failure modes of the Chambercore structure. The main failure modes consisted of compressive buckling and separation between the face sheets and the cells. Buckling initiated at the ribs or at the face sheets depending on the loading conditions. The buckling of the face sheets occurred under longitudinal compressive load but did not lead to immediate failure. The buckling of the ribs occurred under out-of-plane compression at the loading point and lead to the final failure. Separation between the face sheets and the cells was observed at the juncture where a high bending moment was applied under transverse bending and shear loading.

The design of the Chambercore involves designing against buckling and separation at the rib/skin juncture. Buckling can be prevented by proper design of the ply orientation and the cell size. Separation at the rib/skin juncture can be prevented by limiting the bending and shear loads in the transverse direction. Although we need to improve the accuracy of the analysis, we have shown that the finite element analysis can be used for the design of the Chambercore structures. Further study on the input material data and the boundary conditions should close the gap between the analysis and the experiments.

Appendix 1

Load-deflection and load-strain curves of the first transverse 4-point bending test

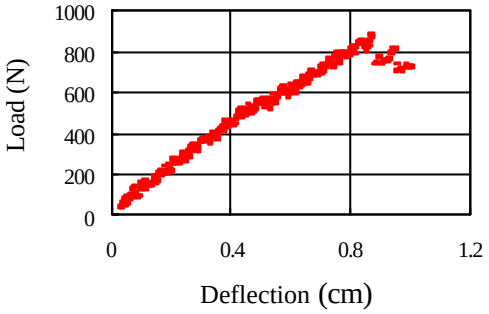

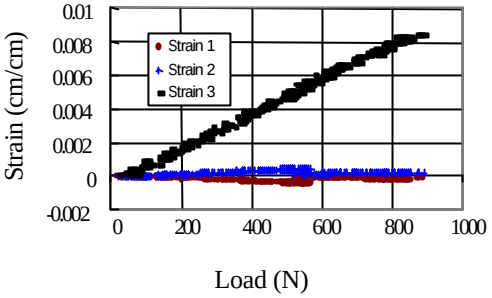

Appendix 2

Picture 1 of transverse 4-point bending test

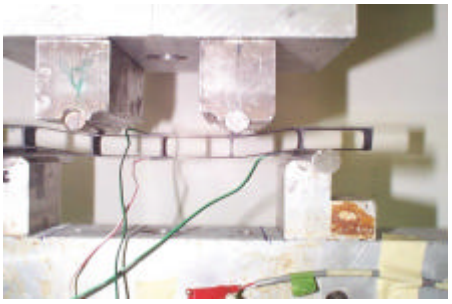

Picture 2 of transverse 4-point bending test

Appendix 3

FEA Model for transverse 4-point bending test

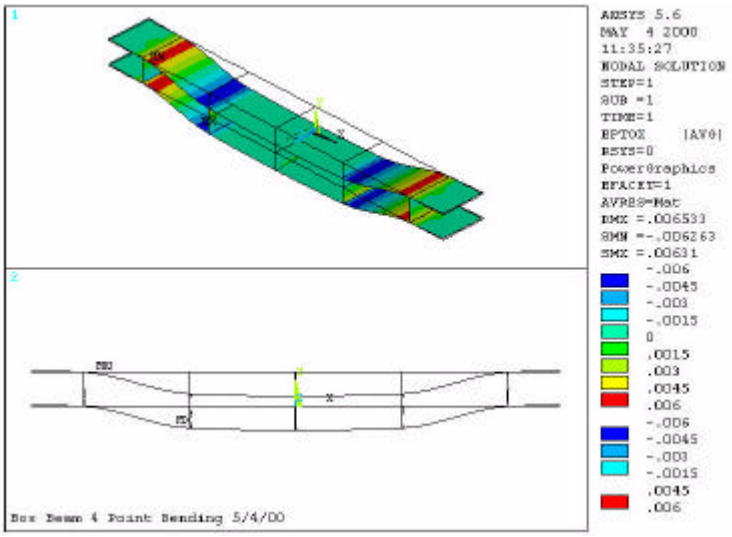

Appendix 4

Load-deflection curve of the first short lengthwise 4-point bending test

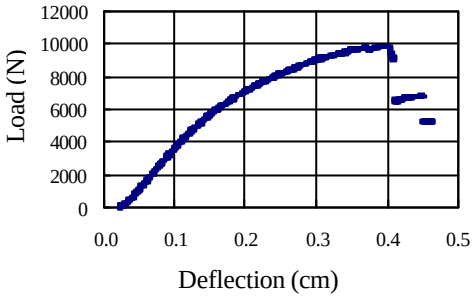

Appendix 5

Picture of the first short lengthwise 4-point bending test

Appendix 6

FEA model for short lengthwise 4-point bending test

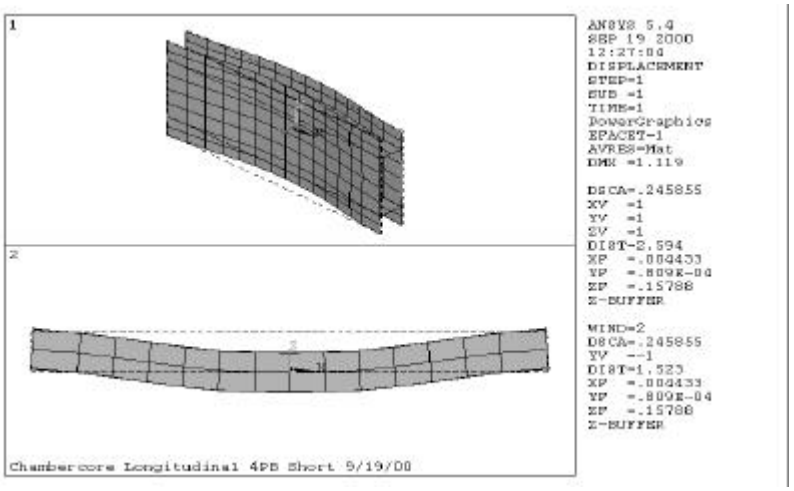

Appendix 7

Pictures of Compression/buckling test

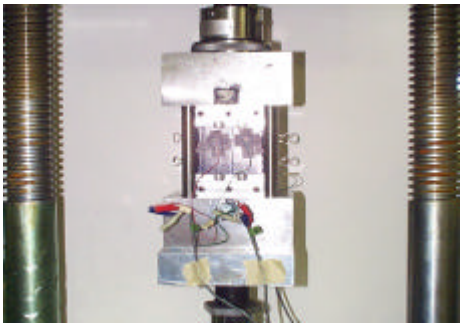

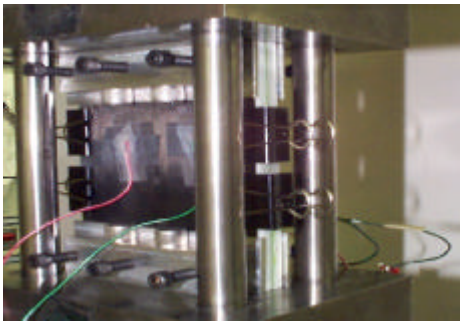

Appendix 8

FEA model for compression/buckling test

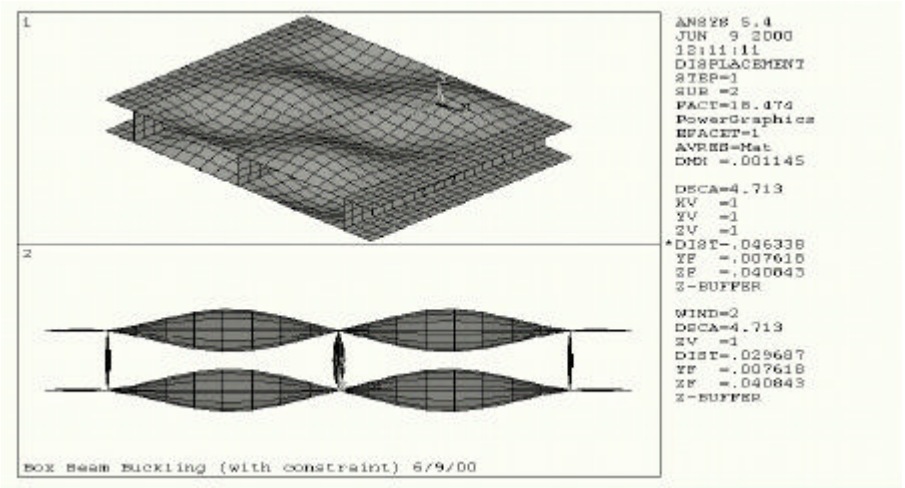

Appendix 9

Load-displacement curve of compression/buckling test

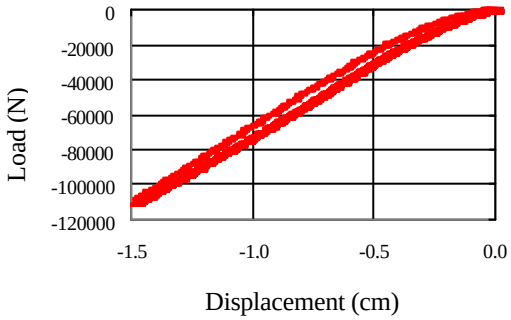

Appendix 10

Load-strain curves of compression/buckling test

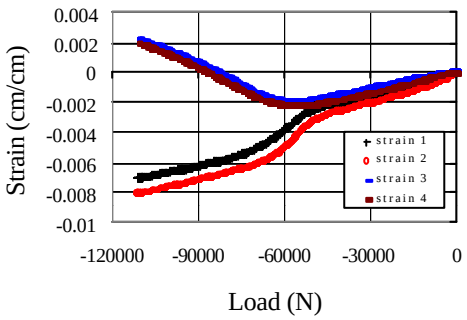

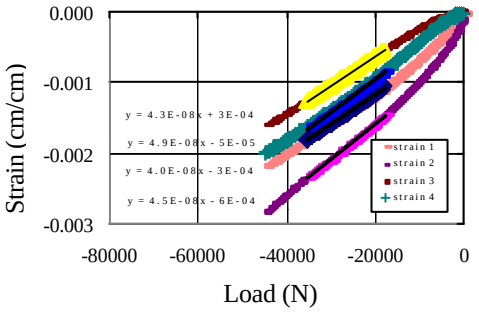

Appendix 11

Pictures of the long lengthwise 4–point bending test

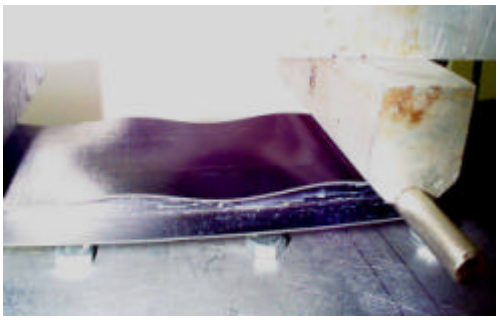

Appendix 12

Load- deflection curve of the first long lengthwise 4-point bending test

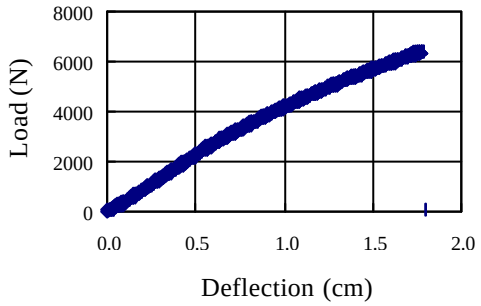

Appendix 13

Strain-Load curve of the first long lengthwise 4-point bending test

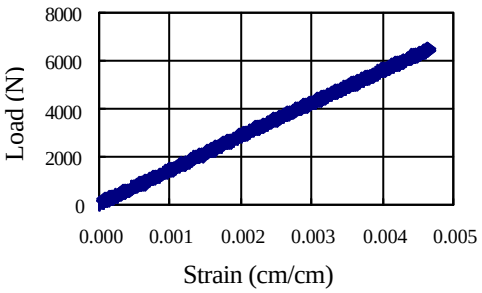

Appendix 14

FEA deflection model for long lengthwise 4-point bending test

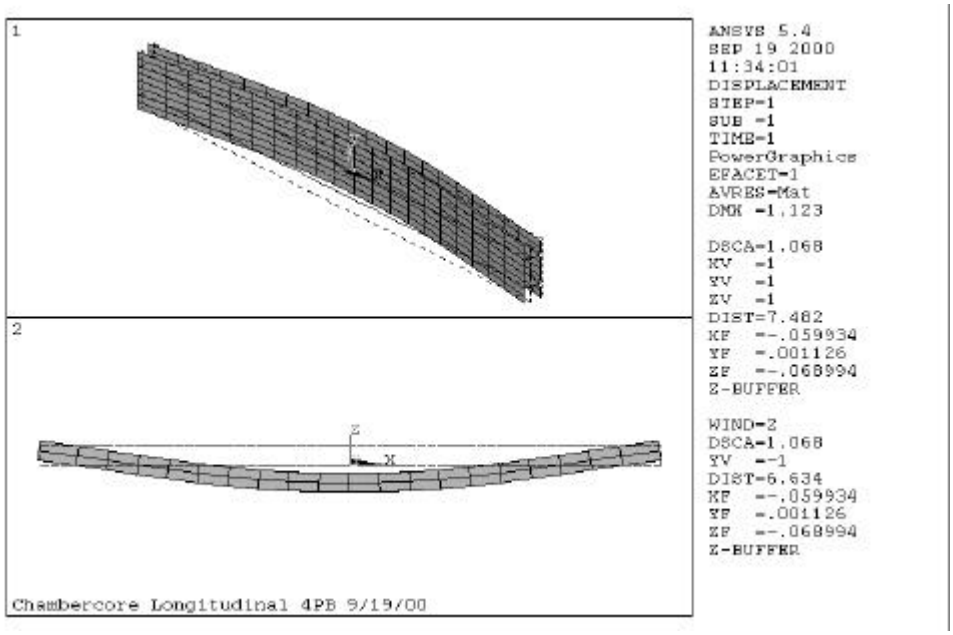

Appendix 15

FEA buckling model for long lengthwise 4-point bending test